Journal of Hydrology 405 (2011) 171–181

Contents lists available at ScienceDirect

Journal of Hydrology

journal homepage: www.elsevier.com/locate/jhydrol

A very large dew and rain ridge collector in the Kutch area (Gujarat, India)

G. Sharan [a,b], O. Clus [b,c], S. Singh [a], M. Muselli [b,c,*], D. Beysens [b,d,e]

[a] DA Institute of Information and Communication Technology, Gandhinagar 382007, India
[b] OPUR International Organization for Dew Utilization, Paris, France[1]
[c] Université de Corse, UMR CNRS 6134, Route des Sanguinaires 20000 Ajaccio, France
[d] ESEME, Service des Basses Températures, DRFMC/DSM/CEA-Grenoble, 17 rue des Martyrs, 38054 Grenoble Cedex 9, France
[e] ESEME, Laboratoire de Physique et Mécanique des Milieux Hétérogènes, ESPCI-Universités Paris 6 – Paris7, 10, rue Vauquelin, 75231 Paris Cedex 5, France

ARTICLE INFO

Article history:
Received 4 November 2010
Received in revised form 16 April 2011
Accepted 14 May 2011
Available online 20 May 2011
This manuscript was handled by K. Georgakakos, Editor-in-Chief, with the assistance of Dr. Noah Knowles, Associate Editor

Keywords:
Dew harvesting
Dew plant
Water resource
Computational fluid dynamics
Radiative cooling

SUMMARY

The world's largest dew and rain collecting system, comprised of ridge-and-trough modules, was constructed in March 2006 at Panandhro in the semi-arid area of Kutch (NW India). The main goals were (i) to collect dew on a scale that could be beneficial to the local population (ii) to determine the efficiency of this new module shape, (iii) to determine whether results obtained from small measurement condensers can be projected to large condensers, (iv) to apply a computational fluid dynamic simulation to improve the condenser set-up. Preliminary studies performed with four standard plane condensers of 1 m^2 surface area, inclined 30° from horizontal, identified Panandhro as a promising site. The cumulated dew water during 192 days was 12.6 mm with a maximum of 0.556 mm/night. A large dew condenser (850 m^2 net total surface) was designed with 10 ridge-and-trough modules. The ridges are trapezoidal, 33 m long, 0.5 m wide at the top, 2.2 m wide at the base and sloping 30° from horizontal. The depth of the troughs between the ridges is 0.5 m. A 2.5 cm thick polystyrene foam rests on the surface as insulation with a radiative foil on top (similar to that developed by OPUR, see www.opur.fr).

Numerical simulations using the computational fluid dynamic software PHOENICS were performed. The most profitable orientation was with the condenser oriented back to the wind direction, a configuration that lowers the wind velocity near the foil due to the combination of free convection and wind recirculation flows.

A comparison of water yields over one year of measurements between four 1 m^2 plane condensers and a 850 m^2 ridge condenser showed a 42% lower yield on the large condenser. The difference is attributed mainly to folds in the plastic foil allowing water to fill the central ridge, thus decreasing radiative cooling. The output for 2007 was 6545 L, corresponding to 7.7 mm/day on average. The largest event was 251.4 L/night (0.3 mm). Such a condenser can also collect rain (and, to a lesser extent, fog). Chemical and biological analyses showed that dew water, once filtered and bottled, could be used for drinking after a light treatment to increase the pH. The price of this water could be lowered to reach 30% (dew only) or even 3% (dew plus rain) of the market prize.

1. Introduction

Dew collecting has the potential to serve as a renewable complementary source of potable water for arid or isolated areas. Systematic investigations of high yield radiative materials with hydrophilic properties for drop recovery and adapted condensing architecture have been performed in the last decade. One such material consists of a white low density polyethylene film including micro-particles with high infra-red emissivity (Nilsson, 1996; Clus, 2007; Organization for Dew Utilization, OPUR). The film is placed on a thermally insulated material and cools below the air dew point temperature through radiative losses. The maximum dew yield measured with plane condensers has been in the order 0.6 mm (Berkowicz et al., 2004; Clus et al., 2009). These values are close to the expected maximum dew yield 0.8 L/m^2 (Monteith, 1957; Monteith and Unsworth, 1990; Garratt and Segal, 1988; Beysens, 1995, 2006). Dew yields can be correlated with local meteorological parameters (windspeed, wind direction, relative humidity, etc., Nikolayev et al., 1996; Nilsson, 1996; Muselli et al., 2002, 2006a; Sharan and Prakash, 2003; Beysens et al., 2003, 2006; Berkowicz et al., 2004; Clus et al., 2006, 2008, 2009; Gandhidasan and Abualhamayel, 2005).

Interest in dew in the Kutch region of northwest India developed from observations that dew occurred frequently over a span

* Corresponding author at: Université de Corse, UMR CNRS 6134, Route des Sanguinaires 20000 Ajaccio, France.
E-mail addresses: girja_sharan@daiict.ac.in (G. Sharan), clus@univ-corse.fr (O. Clus), shashank@purdue.edu (S. Singh), marc.muselli@univ-corse.fr (M. Muselli), daniel.beysens@espci.fr (D. Beysens).

[1] www.opur.fr.

0022-1694/$ - see front matter © 2011 Elsevier B.V. All rights reserved.
doi:10.1016/j.jhydrol.2011.05.019

of several months including the warmer periods. Initial measurements of daily dew volume were made by an improvised method of channeling condensation from the roof of a plastic greenhouse into a bucket placed at the base (Sharan and Prakash, 2003; Sharan, 2006). The Kutch climate is under the influence of the monsoon cycle, with 15–20 rain events from July to mid-September and a long dry season. Dew events occur more frequently (about 100 nights) from late September to early May, with larger yields in spring (Sharan et al., 2007a,b). During the remaining months, the monsoon season makes the sky cloudy and unsuited for dew formation. Chemical tests showed that the dew water of several sites in Kutch is safe and potable. Studies in other parts of the world found that dew water is potable once disinfected (Muselli et al., 2006b; Beysens et al., 2006; Lekouch et al., 2010).

Small prototypes were tested in Kutch followed by larger units (Sharan and Prakash, 2003; Sharan, 2006; Sharan et al., 2007a,b). Three different models were developed for large scale applications – condenser-on-roof (COR), condenser-on-ground (COG) and condenser-on-fence (COF). Different structures have also been studied elsewhere (Muselli et al., 2002, 2006a) and roofs condensing dew water have been built and operated successfully (Beysens et al., 2007).

The main objectives of the present study were (i) to evaluate the yield of ridge-and-trough modules, (ii) to determine whether one can extrapolate results obtained from small condensers to very large dew condensers, (iii) to apply a computational fluid dynamic (CFD) simulation to help design a more efficient condenser set-up. Panandhro (23°40′N, 68°46′E, 42 m a.s.l.) lies within 20 km from the Arabian Sea on a gulf, in the extreme West of the Rann of Kutch and near the city of Bhuj in the state of Gujarat. Precipitation is often low. For example, the cumulative rainfall from February 7, 2004 to January 12, 2005, was only 190 mm. Water must be pumped from deep tubewells and a huge dam situated 7 km west of Panandhro provides fresh water by trucks for the Gujarat Mineral Development Corporation (GMDC) lignite mine, the nearby thermal power plant (Gujarat Electricity Board), the Panandhro village and surrounding villages. This water needs additional treatment to meet international World Health Organization (WHO, 2011) recommendations, but for financial reasons communities in general do not have access to such a water quality level. On April 20, 2006, the dam was empty and the region entered a critical water scarcity situation.

2. Materials and methods

2.1. Planning and Set-up

The dew condenser-on-ground (COG) installation at Panandhro (Fig. 1) was commissioned by the Gujarat Mineral Development Corporation (GMDC) mining company. GMDC's interest in dew collection stemmed from the need to provide irrigation water for vegetation planted over land that had been mined and backfilled. Transporting water was increasingly difficult and expensive. They also expressed interest in using dew to supplement drinking water supply in offices and residences. Accordingly, a large collecting facility was desired. Although residents of the area stated that dew occurred frequently, there was no quantitative data on frequency and magnitude. A set of four OPUR type 1 m^2 condensers, hereafter referred to as planar units, were installed so that one could face each direction. Such units are described in detail elsewhere (see Nilsson, 1996, and www.opur.fr). Daily measurements commenced in October 2005 and every week the dew observations at Panandhro were compared with measurements made in parallel

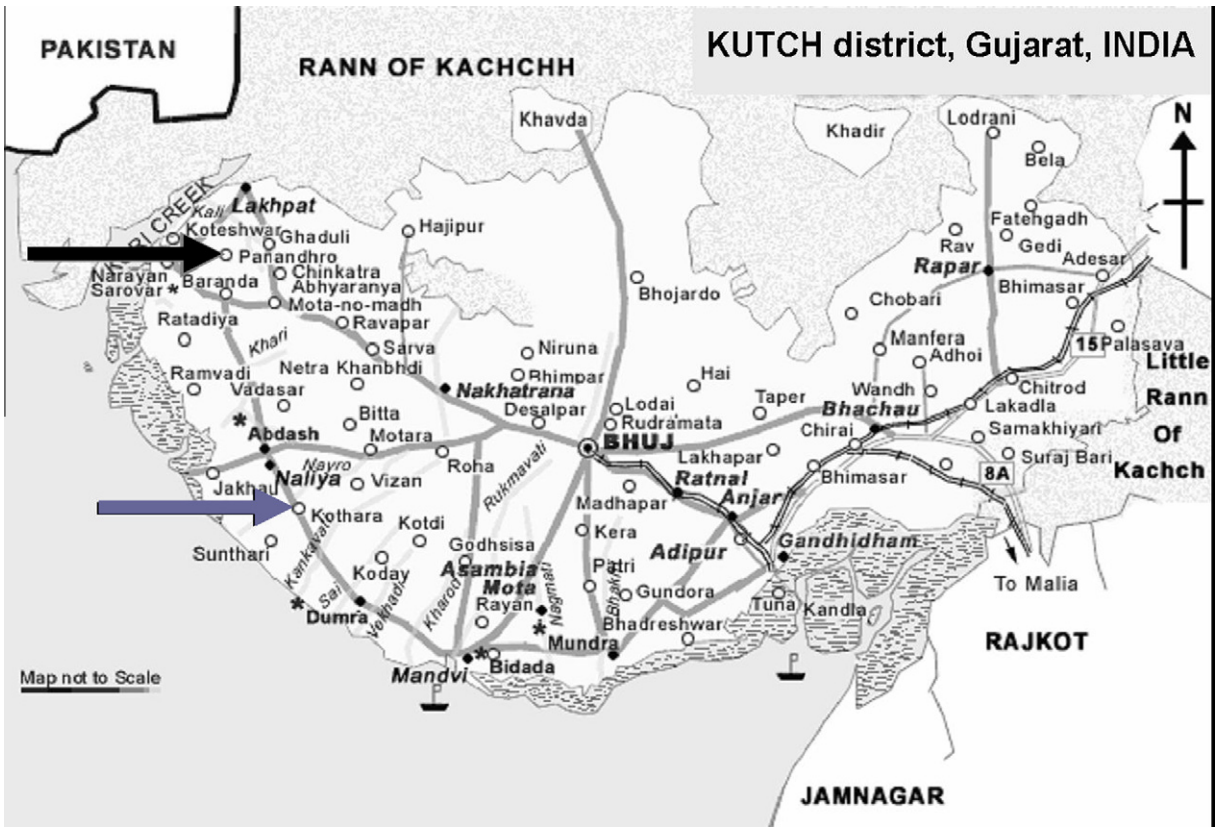

Fig. 1. The region of Rann of Kutch (northwest India). Black arrow indicates the GMDC mine of Panandhro, gray arrow indicates the Indian Institute of Management at Ahmedabad Development and Outreach Station in Kothara.

70 km away at Kothara (Fig. 1) using identical condensers similarly oriented. Kothara is the center of a dew condenser research project and daily dew water measurement had been carried out for several years. By February 2006 it became apparent that the frequency and pattern of occurrences were similar at the two sites, though the magnitude appeared to be slightly lower in Panandhro. This was confirmed when one full year (2007) of data was available (16.5 mm yield, see Sections 4.1 and 4.2, below, for more information). The questions addressed next were what type of facility would be best, i.e. a condenser-on-roof (COR), condenser-on-frames (COF), or condenser-on-ground (COG), and how large should the facility be in terms of condensing surface area?

Although the CORs and COGs are cheaper to install per unit area as no extra support or mounting is required, there are drawbacks. Size is constrained by the roof area, pitch is often less steep than required (30°) for dew collection, elevation is higher than optimal and orientation unchangeable. The largest working COR type system built in the area at the time had an area of 360 m^2 (Sharan et al., 2007c). The dew yield was nearly 50% of the yield from the 1 m^2 measuring units mounted on frames. Nevertheless, the water from COR was an appreciable amount for the users and it required only a small investment to build the facility. The possibility of building CORs at the Panandhro site did exist with numerous sheds with large roof area, housing offices, garages, repair workshops and warehouses but these were not favored because the roof pitch was 15–20°, and higher wind speeds would adversely affect yield. Extra costs would be required in water conveyance and collection from several distributed units. Another option considered but not favored was to mount a condenser surface using an iron framework. The reasons were that a metal framework was expensive and would degrade rapidly in a corrosive coastal environment. Metal frame supports could be used for small measuring condensers. Accordingly, a condenser surface situated directly on the ground offered the best option since land was of low value and without an economically attractive alternative use. There would be no constraint on the size; a condenser-field could be as large as required and expanded in future.

At the time, limited experience was available on COG type units at Kothara where three experimental units each 9 m^2 (3×3 m) were under investigation. Units were separate but placed adjacent to each other. All three were identical in construction, built over a bed of sandy soil, facing east, and inclined 30° from horizontal. All three were set against a 2 m high boundary wall. The condensing surface was made of the same film as the 1 m^2 planar units and similarly insulated. Data from all three condensers pooled and averaged over two consecutive seasons showed a yield of 16.1 mm. During the same two seasons the east-facing small condenser unit located 500 m away yielded 19.4 mm. This indicated that the output of COG may be ~15% lower than that obtained from small condensers on frames. Despite this it was decided to shape the large condenser directly on the ground (Fig. 2) due to the advantages mentioned above. It was also decided that the condenser field would have a ridge-and-trough architecture (not smooth planar), with the ridge walls (condensing faces) inclined optimally and only 100 cm in length as in the small condenser unit. This would also make it easier to access the entire surface for cleaning. The COG was built to be about 900 m^2 in area and, to our knowledge, this facility was the largest in size and unique in architecture. The performance of COGs of such a large size and with such an architecture had not been studied before. The project

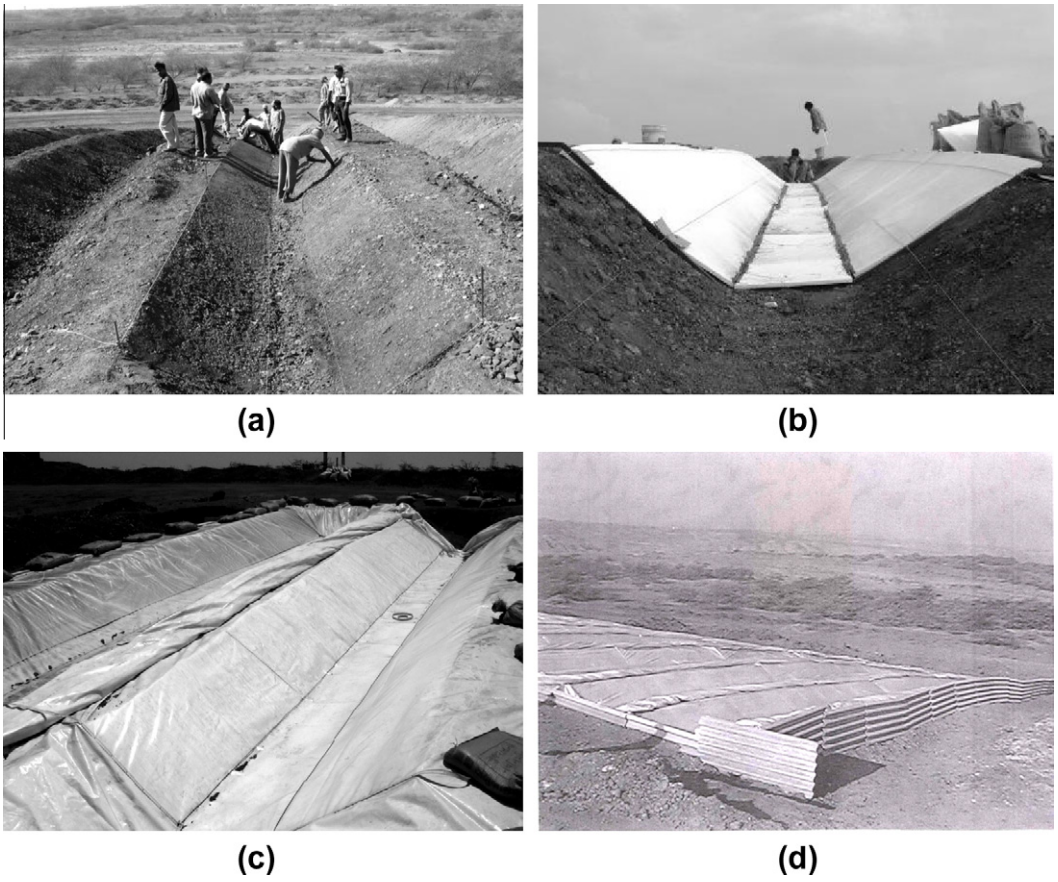

Fig. 2. Erection of the first ridges. (a) Ground shaping; (b) foamed polystyrene insulation; (c) Foil placement; (d) Overview of the first 10 ridges (850 m^2) from the top of the hill. Note that the top of the ridge contributes very little to dew water.

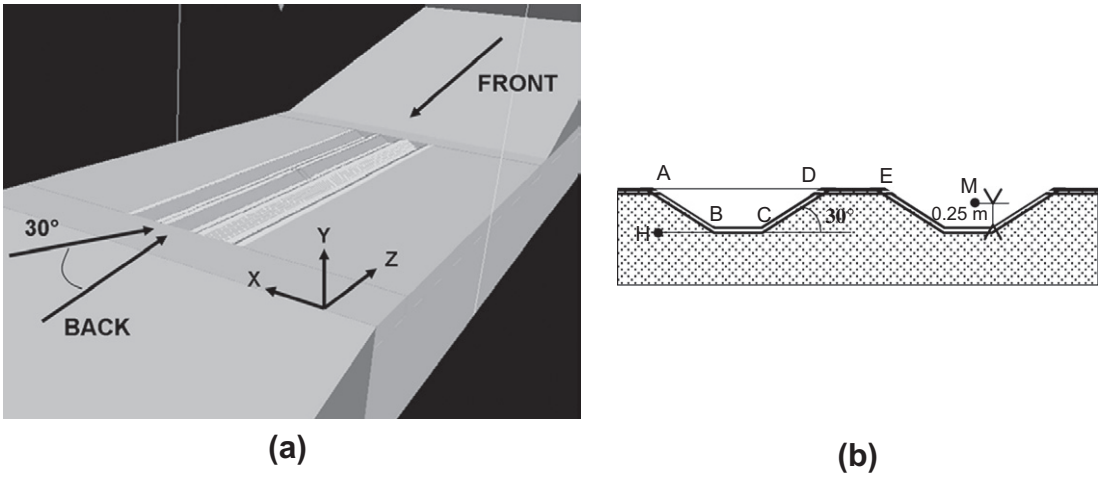

Fig. 3. (a) Sketch of the modeled condenser composed of three 33 m ridges long on a 40 m long slope tilted 15° from horizontal. The origin of the axes is at the top of the ridges. (b) Section of the ridge. AB = CD = 1 m; BC = DE = 0.5 m, AH = 0.5 m (depth).

thus provided an opportunity to do so and to compare it with smaller units installed side by side. Modeling and simulation of the ridge-and trough condenser using CFD was carried out to determine insights into possible factors that drive cooling and condensation on such surfaces. Establishing a quantitative relation between yields from large and small units is not only of scientific importance but also of practical use in engineering design and sizing of working systems for a given or desired output.

The installation site provided by GMDC is situated on a 1740 ha plot of land that had been mined (of lignite) and backfilled. A 15° and 40 m long slope was planned on a hillslope 300 m in overall length and facing NW (300°). Details of the construction can be found in Clus et al. (2007). The main features are described here in brief.

The installation consists of three parts – a condenser field to produce water, a conveyance and storage unit to collect and hold the water, and a protective boundary fence able to keep runoff water from entering during rains. The basic unit shape is a trapezoidal ridge, formed on the ground – 220 cm at the base, 50 cm at the top and with two side walls each 100 cm long inclined at a 30° angle (Figs. 2a and 3). This angle is close to the limit of natural dune surface stability and is also the "best" angle to enhance dew droplet recovery by gravity while not diminishing the radiative cooling, as demonstrated by Beysens et al. (2003). This form was selected (over others) to make the facility compact and to provide more condensing area per unit land area. The ridge surface is lined with a 2.5 cm thick styrene foam insulation and covered on top with a special plastic film (Figs. 2b and c and 3b). Longitudinally the ridge has a slope of 15°. Condensation occurs principally on the two walls and then flows longitudinally down the base into a common gutter at the lower end. The condenser field is composed of 10 parallel ridges adjacent to each other (Fig. 2d). Each ridge is about 32–35 m long. As the top of the ridge is flat, it contributes very little to dew water and can be ignored in calculating the condensing surface area. With a width of 2.5 m, the model ridge has a surface area of 82.5 m^2 (TS). The horizontal projected area is 73.6 m^2. The total condensing surface area is 850 m^2. It can be expanded by adding more ridges when needed. Material used in constructing the condenser field included plastic film (approximately 1000 m^2), 1000 styrene foam boards each 1 $m^2 \times 0.025$ m), UV stabilized ribbon, wooden batons and 100 kg of molten tar. Dew water conveyance and storage was made with 20 m long, 15 cm diameter diameter PVC pipes, connector tees and elbows, and filter screen fittings to prevent dust and straw particles from entering the common gutter. Water storage was a 3000 L tank. A protective boundary fence to prevent runoff water from entering during rains was erected using 3 m × 1 m cement-asbestos sheets (Fig. 2d). The total cost of installation, excluding labor, was approximately US$3100. Of this, the condenser-field accounted for US$2100 (film US$1000, insulation boards US$1000, ribbon batons and screws US$100), water conveyance and storage US$500, fencing US$300, and land-shaping US$200. The plastic film is UV stabilized with a normal life of 3–4 years; the insulation boards, batons, water conveyance and fence are expected to last 10–15 years.

2.2. Meteorological data

Meteorological data were obtained from the meteorological station of the Gujarat Electricity Board's (GEB) power plant, situated 2 km southeast of the site. Data were available for the period from February 7, 2004 to February 25, 2006 but with data lost for 25% of the measurements days, and all of 2007. Measurements included air temperature (T_a, °C) with an accuracy ±0.2 °C (resolution ±0.1 °C), relative humidity (RH, %) with an accuracy of ±3% (resolution ±0.1%) and rain (h, mm) with an accuracy of ±0.1 mm. Wind speed (V, m/s) with an accuracy better than ±0.5 m/s, stalling speed 0.3 m/s, and wind direction (accuracy 3°, resolution 1°) were measured at 4.1 m above the ground. Windspeed was extrapolated at z = 10 m height by using the classical logarithmic variation (see e.g. Pal Arya, 1988):

$$V(z) = V_{10} \ln(z/zc) / \ln(10/z_c), \quad (1)$$

where z_c (taken here to be 0.1 m) is the roughness length.

Fog incidence is not recorded by meteorological offices because it is very rare (3 or 4 days per season).

3. Numerical simulations

3.1. Background

The aim of the numerical simulation was to determine the dew water output expected from COG at Panandhro for an optimal orientation with respect to the mean wind direction. A radiative condenser is basically a thermal machine whereby three main characteristics must be simulated, (i) the radiative material thermal properties (thickness, heat conductivity, heat capacity), (ii) the radiative cooling power, function of the atmospheric conditions (T_a, RH, cloud cover), the condenser exposure and its shape, and (iii) the incoming diffusive and convective (free or forced) heat,

the value of which is a function of the windspeed and the condenser architecture. The surface to air heat transfer coefficient was determined analytically only for planar surfaces with laminar air flow (Nikolayev et al., 1996, 2001) and for adding free convection (Jacobs et al., 2008). For more complex surfaces, a semi-empirical description is needed (Guyer and Brownell, 1999). As a consequence, the analytical description of dew condensation in complex structures subject to outdoor natural wind is extremely difficult. Moreover, dew condensation occurs frequently with weak wind and the free and forced (wind) convections can be of a comparable order of magnitude. The relation between a 10 m meteorological wind and the local air flow tangential to a surface making a variable angle with horizontal α has already been simulated by Beysens et al. (2003). The main result was that the tangential velocity is found to be at a minimum when $\alpha \approx 30°$.

Numerical experiments using PHOENICS computational fluid dynamics (CFD) software have been developed as a complementary tool that can be included in the various steps of the condensation process (Clus et al., 2006, 2009; Clus, 2007). The main contribution of CFD is to solve the system by including material properties, radiative cooling, and convective heating by way of iterative calculations using a numerical code. The comparison of structures behavior at different wind speeds permits the visualization of new condenser shapes and estimations of the effect of scale change, from small prototypes to large scale installations (Clus et al., 2009).

The analysis of meteorological data as compared to the dew yield is outlined below in Section 4.2. An important result concerns the mean windspeed $\overline{V}_{10} \approx 1.5$ m/s and average direction 210° during dew events. All calculations were carried out for standard weather conditions during nocturnal dew events: clear sky, $T_a = 288.15$ K (15 °C), $RH = 80\%$. These conditions correspond to a dew point temperature $T_d = 11.8$ °C. Standard numerical values were used for the air properties (density, thermal conductivity, specific heat, etc.).

3.2. Radiative cooling

Imposing a specific radiative cooling power to the condenser is not possible in the *PHOENICS* program as it is a pure surface property. We thus convert the surface cooling power into a uniform volumetric heat flux using an approach (Clus et al., 2009) whereby the following reduction laws must be respected between each elementary unit of the virtual material (thickness e_c [m], volume heat capacity C_c [J K^{-1}], thermal conductivity k_c [W m^{-1} K^{-1}]) and the corresponding unit of the actual material (thickness e_M, volume heat capacity C_M, thermal conductivity k_M).

The conservation of heat capacity per unit surface is:

$$C_M e_M = C_c e_c. \tag{2}$$

and the conservation of the heat flux component perpendicular to the material is:

$$\frac{k_M}{e_M} = \frac{k_c}{e_c}. \tag{3}$$

At a solid–fluid interface, the heat flux q (W m^{-2}) can be related to the difference between the temperature at the interface and that in the fluid, $q = h(T - T_{fluid})$. This expression, sometimes called the Newton's law of cooling (Bird et al., 1960), is more a definition of the heat transfer coefficient h (W m^{-2} K^{-1}) rather than a law. However, by applying this "law" in series we can obtain an equivalent thermal conductivity. This can be used for a series of neighboring solids of various thicknesses, with one or two extremities in contact with a fluid.

The correction for the thermal conductivity is isotropic and thus increases the heat flux components parallel to the condenser surface. This establishes an artificial homogenization of the temperature in the volume of the condensing material. However, in the present study, we limit ourselves to the surface temperature because we only need to study the differences between the condenser surface temperatures to that of the ambient air temperature.

The power emission law of each cell of the "virtual radiator" is a function of its local temperature and is determined with a specific integration program (Clus et al., 2009) that is summarized here. The relative cooling power is the difference between the radiator emissivity and the sky radial emissivity that depends on the angle θ (°) with the zenith. The incoming angular sky long wave radiation dIR_Ω (W/m^2) in an elementary solid angle $d\Omega$ is modeled following:

$$dIR_\Omega = \varepsilon_\theta \cdot \sigma \cdot T_a^4 \cdot d\Omega/\pi. \tag{4}$$

Here,

$$\varepsilon_\theta = 1 - (1 - \varepsilon_{total})^{1/(b\cos\theta)}, \tag{5}$$

is the angular emissivity (Berger and Bathiebo, 2003), σ is the Stefan–Boltzmann constant, T_a is the ambient temperature measured at the ground level (fixed at 288.15 K for the simulations) and ε_{total} is the relative sky emissivity, estimated here to be 0.8, a reasonable value for an air with 80% *RH* (Nikolayev et al., 2001). The angle emissivity θ is the angle relative to the zenith (vertical) direction and $b = 1.66$ (Berger and Bathiebo, 2003). The condenser is taken as a gray body with emissivity 0.94 (Nikolayev et al., 2001) for calculating the angular long wave radiation emitted in the solid angle $d\Omega$. The radiative budget is then integrated over the hemispherical sky and the radiator.

3.3. Results

The Panandhro site was modeled in 3 dimensions according to Fig. 3. Only three identical ridges were integrated in order to limit the number of cells and the time calculation. The results analyzed were collected only on the central section AD in order to remove lateral edge effects.

Three wind directions were considered; perpendicularly to the hip edge and from the back of the ridge ("back" wind on Fig. 3a), perpendicularly to the hip edge and in front of the ridge ("front"

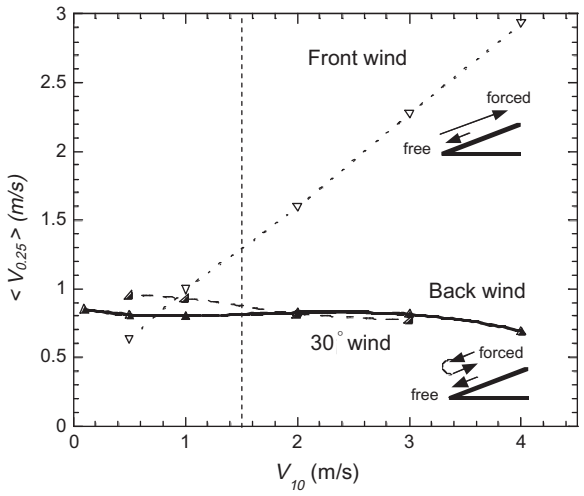

Fig. 4. Airflow velocity $\langle V_{0.25}\rangle$ in the middle of the ridge, in M (see Fig. 3b) at 0.25 m above the bottom surface, with respect to windspeed V_{10}. The data are absolute values averaged over the ridge length. Front wind: open triangles; back wind: black triangles; 30° wind: bent black triangles. The vertical line corresponds to the mean windspeed (1.5 m/s) during the dew events.

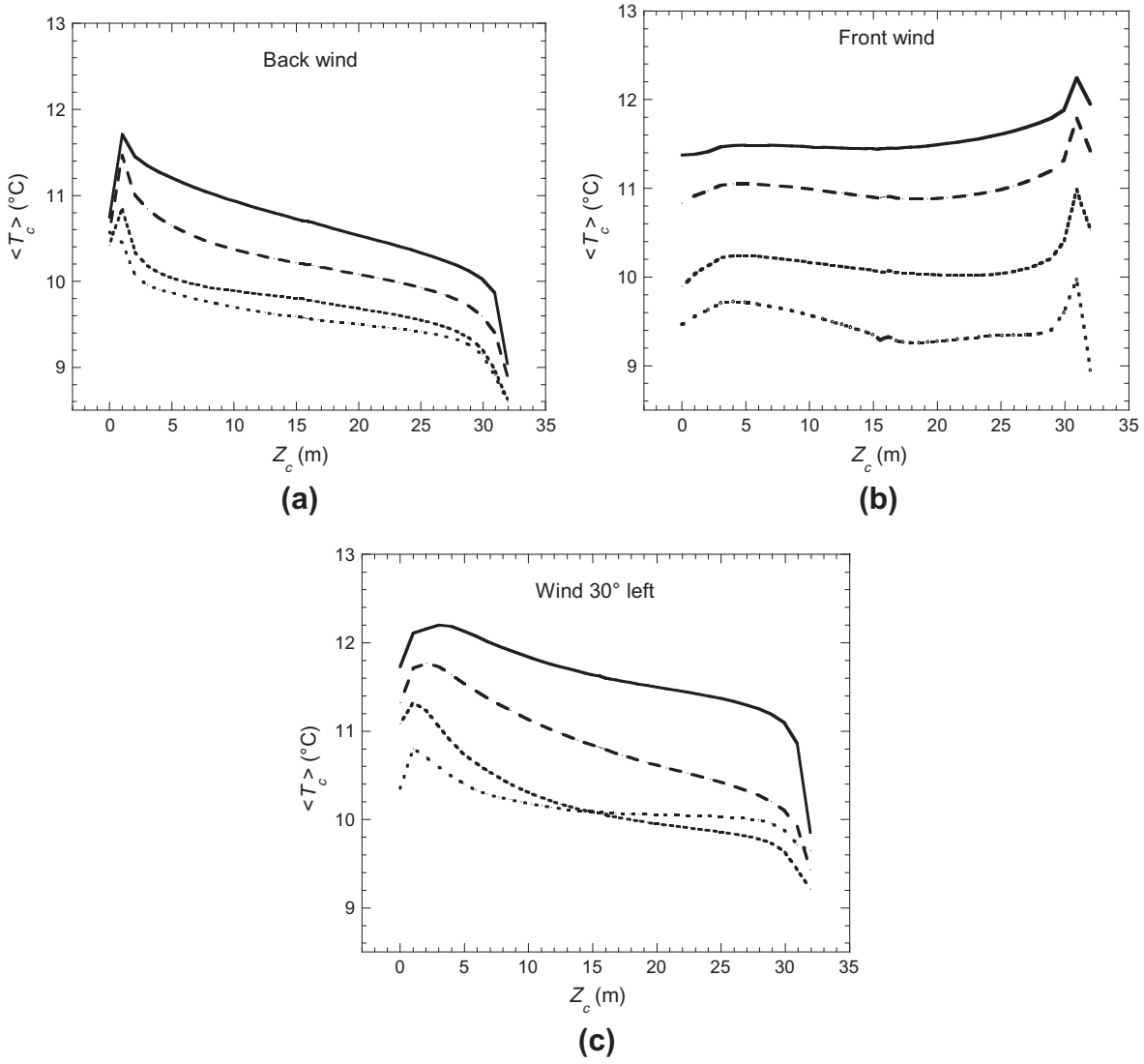

Fig. 5. Variation of the average surface temperature $\langle T_c \rangle$ along the length of the central ridge (Z axis, the origin of axes is at the top of the ridges. see Fig. 3a) for T_a = 15 °C and wind speeds V_{10} = 0.5 m/s (simple dots): 1.0 m/s (bold dots); 2.0 m/s (dash); 3.0 m/s (continuous line). (a) Back wind; (b) front wind; (c) 30° wind.

wind, Fig. 3a), and an intermediate case where the wind makes a 30° angle with the hip edge (wind "30°", Fig. 3a).

3.3.1. Airflows

Fig. 4 shows the result of simulations at various wind speeds for front, back and 30° wind directions. The goal of this simulation was to assess the situation where wind is increased, which in turn increases the convective heat transfer.

The flow velocity $\langle V_{0.25} \rangle$ is averaged along the ridge length at a point M that is situated in the middle of the ridge at 0.25 m above the bottom (see Fig. 3b). The amplitude of the natural free convection is provided for $V_{10} \to 0$. The value $\langle V_{0.25} \rangle$ = 0.85 m/s obtained for V_{10} = 0.1 m/s is representative of this limit. It indeed corresponds to measurements performed in the vicinity of planar condensers (Beysens et al., 2005).

The air flow in the ridge results from the addition of free and forced convection, the latter inducing a back flow at high wind speed values (Muselli et al., 2002; see Fig. 4 inserts).

For back wind direction, the lowering of air flow velocity at large windspeeds can be understood as the effect of the vortex above the hip that counterbalances the free convection, in a way similar to the inclined plane case (Beysens et al., 2003).

The 30° wind configuration provides results similar to the back wind. However, for V_{10} < 1 m/s, the lateral wind convection reinforces the natural convection.

The front wind configuration leads naturally to an increase of $\langle V_{0.25} \rangle$ proportionally to windspeeds for V_{10} > 1 m/s, when free convection becomes negligible. At low windspeed (V_{10} < 0.85 m/s), free convection flows counterbalances the natural wind resulting in a decrease of the airflow velocity.

Looking now at the mean windspeed (1.5 m/s) where dew is observed on 1 m^2 plane condensers, back wind and 30° wind configurations exhibit nearly the same flow velocity, close to free convection. In contrast, the air flow in the front wind arrangement is larger.

3.3.2. Cooling

From the simulation the temperature contour picture of the ridges can be obtained. In order to compare cooling at different wind speeds and wind orientations, without lateral edge effects, we only consider the variation (along the Z axis) of the temperature $\langle T_c \rangle$ along the central ridge (Fig. 5). $\langle T_c \rangle$ represents the mean surface temperature of a section of the two 30° tilted faces of the ridge: $\langle T_c \rangle = 1/2\ [\langle T_c(\mathrm{AB}) \rangle + \langle T_c(\mathrm{CD}) \rangle]$. $\langle T_c \rangle$ varies appreciably along the ridges and depends noticeably on the wind direction.

The longitudinal temperature variation generates interesting edge effects. For example, with wind from the back with a wind speed of 0.5 m/s, the mean temperature of the ridge surface on the side from which the wind arrives is 10.7 °C, declining to 8.6 °C at the end of the ridge (33 m). The edge effects are then noticeable, $\langle T_c \rangle$ being higher on the side where the wind hits the ridge. With increased speed, the overall patterns and the effect remains similar but the degree of cooling is less. The cooling efficiency logically shows the same characteristics as discussed with the air flows in the above section. These edge effects may explain why it may be inaccurate to use measured dew yield per unit area of small (1×1 m) condensers to estimate yield from a geometrically similar larger unit by simply multiplying by area.

For the condenser temperature $\langle T_c \rangle$ averaged on the whole ridge length, a factor of relative cooling efficiency (or "temperature gain") Δ_T can be defined (Beysens et al., 2003) for various orientations of the system:

$$\Delta_T = \frac{T_c - T_a}{T_{ref} - T_a} \tag{6}$$

Here T_a = 15 °C and T_{ref} stands for the mean condenser temperature when the wind is from the back. Fig. 6 displays the temperature gain variation in relation to the wind direction. The cooling efficiency exhibits the same characteristics as discussed with the air flows, and three regions can be distinguished:

(i) $V_{10} = 0$. The values were calculated by performing simulations at V_{10} = 0.1 m/s and extrapolating to zero. All wind configurations give the same result as the heat exchange is now only due to natural convection with mean velocity $V_{0.25}$ = 0.85 m/s (see above).
(ii) $V_{10} \geqslant 1$ m/s. Natural convection becomes negligible with respect to the atmospheric wind and then surface cooling decreases with windspeed. The 30° wind and the front wind configurations give nearly the same temperature gain, that is a lower degree of cooling than when the wind is from the back. The only exception is for the back wind configuration where the windspeed is notably reduced on the ridges and where cooling is more efficient.
(iii) $0 < V_{10} \leqslant 1$ m/s. The atmospheric windspeed is lower or in the order of the natural convection (≈0.85 m/s). Cooling depends crucially on the exact wind configuration. The behavior for the 30° wind configuration exhibits a local minimum. Cooling is less efficient between 0.5 and 1 m/s, a result that can be understood by lateral edge effects. This effect would be certainly lowered if the full condenser (10 ridges) would have been simulated.

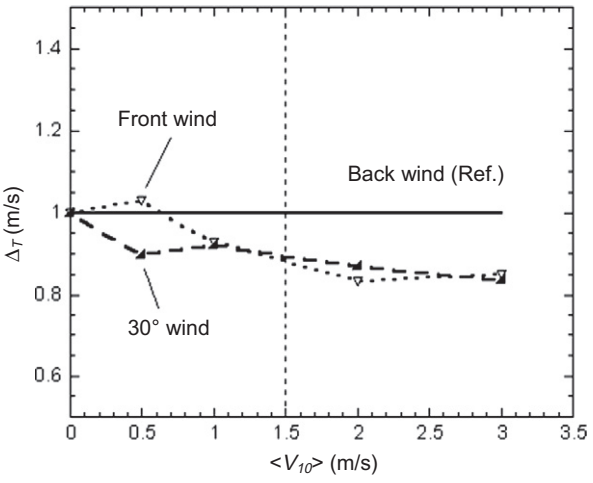

Fig. 6. Temperature gain (see Eq. (4)) with respect to windspeed V_{10} for three simulated configurations: front, back and 30° wind. The back wind configuration is taken as the reference. The vertical line corresponds to the mean windspeed during dew events (1.5 m/s).

In the case of back wind configuration, natural convection and atmospheric wind flow in the same direction, the same air is cooled when flowing on one ridge from top to bottom. A paradoxical result was found for the front wind configuration where cooling is larger than for zero windspeed. As noted above, in this particular arrangement the natural convection flows in the opposite direction to the atmospheric wind, thus reducing the air flows and increasing cooling.

As the temperature gain Δ_T is well correlated with the dew yield (Clus et al., 2009), it therefore appears that the orientation back to the mean wind direction during dew events (210°) is the most favorable orientation for enhancing dew yields. Such an arrangement should increase the dew yields from 10% to 20% for wind speeds >1 m/s (Fig. 6).

4. Dew yields

4.1. Plane condenser data

Dew water from each of the four 1 m^2 units was collected in a plastic bottle attached to the unit and the volume was noted each morning at 08.00 local time. Volume was measured in a graduated glass vessel with an accuracy of ±5 mL (corresponding to ±0.006 mm). Condenser surfaces were not scraped even though some moisture was easily visible at the time of observation and which evaporated shortly afterwards. Clus et al. (2007) reported on results for the period October 8, 2005–April 17, 2006. The dew season runs a few days longer, beginning around the last week of September and ending early May. As reported earlier, the maximum yield was 0.566 mm. The accumulated yields are important, with 12.5 mm for the south-facing unit and 12.6 mm for the west-facing unit. The total accumulation is lower because the measurements did not completely cover the full dew season. In the subsequent full dew season the total measured accumulation was 16.5 mm. Cumulated dew yield already corresponds to 6.6% of the total rainfall (189.5 mm) measured in 2004 in Panandhro (February 7, 2004–January 12, 2005 With a full dew season the dew yield would reach 8.6%. During the measurement period (192 days), the dew events occurred on almost one-third of the nights. The mean yield (maximal for the south- and west-facing units) was about 0.2 mm per dew event. It is noticeable than only one rain event with negligible yield was observed during this dew measurement period.

4.2. Meteorological factors

The dew yield was lowest from mid-November to mid-January (Fig. 7), about 0.06 mm on average per day. In comparison, from October to mid-November, the average dew yield was about 0.08 mm per day and from mid-January to April, the dew yield reached 0.11 mm per day. During the 2004–2005 dew season, the same phenomenon was observed in Kothara during December and January (Sharan et al., 2007a, 2007b). It was attributed to *RH* variations and the seasonal wind regime. The relative humidity decreases after the monsoon period until December and then increases until end of May, when the monsoon starts.

Fig. 8 presents the annual evolution of the main meteorological parameters (*RH*, *V* and wind direction) that drive dew condensation. Four distinct periods can be seen. In Fig. 9 are also contains

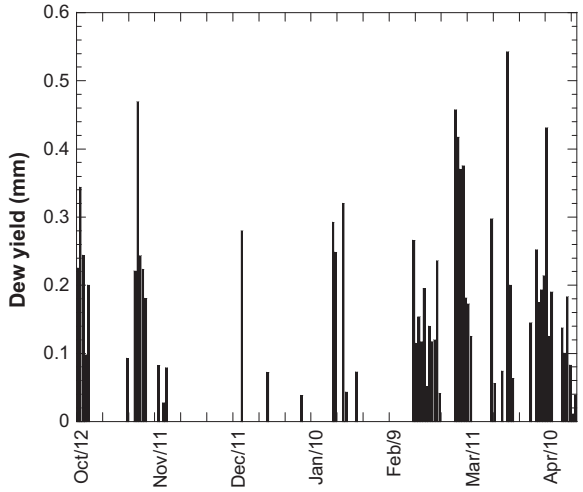

Fig. 7. Distribution of dew yields during the 192 days measurement period, October 8, 2005–April 17, 2006 (averages of the four condensers).

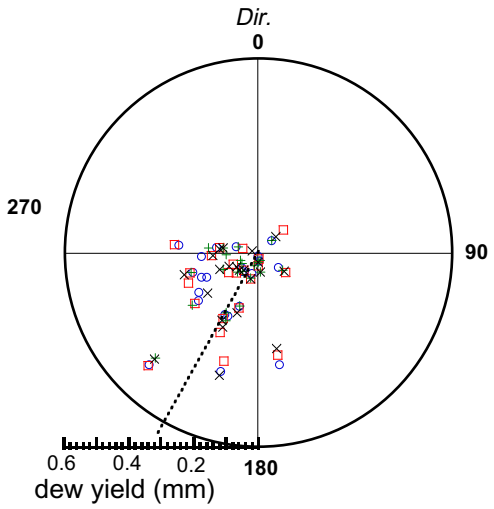

Fig. 9. Dew yields (mm) of the four directional test condensers (×: north; +: east; □: south; ○: west) correlated with night mean wind direction (October 8, 2005–April 17, 2006). The dotted line is the mean wind direction for dew events.

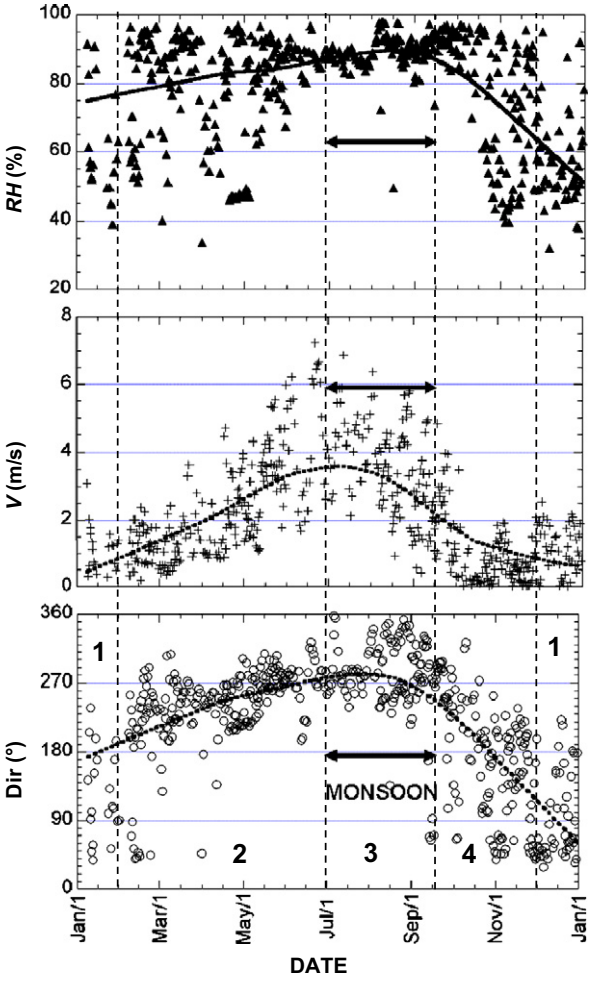

Fig. 8. Relative humidity *RH*, windspeed V_{10} and wind direction. All available data (February 7, 2004–February 25, 2006) are represented on the same one year axis. Data are averaged during the night (from 21:00 h to 7:00 h) and the lines correspond to a 50% weighting of values. The year is divided into four periods labeled from 1 to 4.

the dew yields with respect to wind direction for the four planar 1 m^2 condensers.

From December to February (period 1), the wind is continental and turns from north to south-east. The mean nocturnal windspeed is generally below 2 m/s and the atmosphere is around 60% *RH*, corresponding to the smallest dew yields (see Figs. 7 and 9).

From February to June (period 2), the wind turns to south and west (ocean direction). The windspeed, generally below 2 m/s, increases to about 4 m/s in May. This sea breeze corresponds to a more humid air entry with *RH* commonly above 80%. This period corresponds to the highest dew yields as seen in Figs. 7 and 9.

From mid-July to mid-September (period 3), the monsoon season is characterized by NW strong winds with very high *RH*. However, as the sky is most often cloudy, there are no dew events.

From September to December (period 4), the wind direction returns back to north, with alternative humid south-west wind and dry north-east winds. This season gives high dew yields (Figs. 7 and 9).

Table 1 shows that S- and W-oriented condensers collect approximately 20% more water than N- and E–oriented condensers. Fig. 10 reports the difference in daily dew yields ($h_W - h_E$) between the W-oriented and E-oriented condensers with respect to wind direction and *RH*. It is noticeable that the discrepancy does not come from events corresponding to $RH < 97\%$ where $h_W - h_E$ is negative, but only from a few events corresponding to near 100% *RH*, where condensation in the atmosphere (radiative fog) could form. Fog events, although not documented, can occur in the Panandhro area and the capture of fog droplets is likely to be enhanced on the S- and W- front wind orientated condenser.

4.3. Ridge data

The dew plant was a working installation managed and operated by the owners. It was situated deep inside the mining area accessible only to the company security staff. Organizing accurate daily monitoring of collection by research engineers associated with the project was not feasible (due to security restrictions, remoteness). However, a simple procedure for measuring daily accumulation was made and designated staff of the company were trained to do so. A graduated rod was prepared to easily measure (accuracy ±2 L, corresponding to ±0.0025 mm) the collected water in the collecting tank. Daily measurements were done at 08:00 local time and the ridge surface was left unscraped. From March

Table 1
Dew events and dew yields during 192 days of measurement from October 8, 2005 to April 17, 2006 for each 1 m^2 standard (OPUR type) condenser according to orientation.

Dew days (192 days)	NORTH 69	EAST 73	SOUTH 75	WEST 75
Max. yield (mm)	0.550	0.524	0.566	0.532
Mean yield (mm)	0.169	0.162	0.189	0.189
Cumulative (mm)	11.64	11.79	14.14	14.19
% Of dew days	32.9	34.8	35.7	35.7

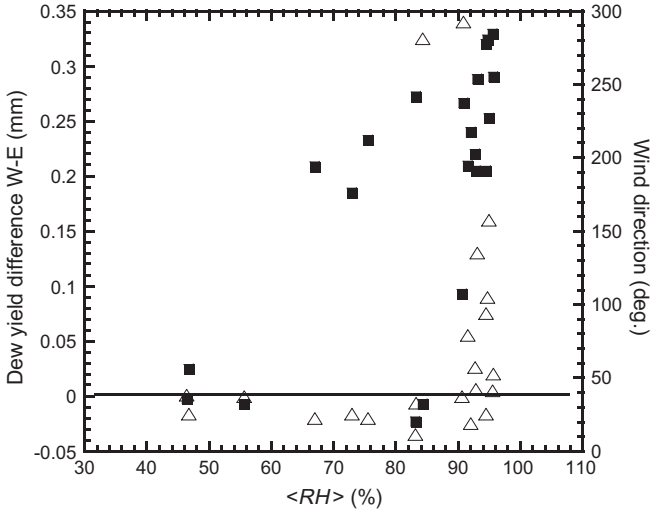

Fig. 10. Correlation of the different dew yields ($h_W - h_E$, mm/night, open triangles) between the W-oriented and E-oriented condensers and wind direction (black squares) with respect to *RH* (%) (data at 05:00 a.m.).

22, 2006 to February 22, 2007, 54 dew events were sporadically measured, initially (March 22, 2006–November 7, 2006) on one ridge only with a net surface area of 85 m^2, but subsequently (November 8, 2006–February 22, 2007) the measurements covered the full 850 m^2 condenser. Beginning 2007, all ten ridges were functional. The total accumulation of dew water from January 2007 to December 2007 was 6545 L, i.e. equivalent to 7.7 mm (Table 2). This does not include yield in December when no measurements could be made due to the absence of staff. Dew occurrence during December is normally similar to that in November. During this period the collection from the 1 m^2 condensers averaged 16.5 mm. The comparison of dew yields measured with the 1 m^2 condensers and the 850 m^2 condenser is given in Fig. 11 where is reported the cumulated dew volume by class amplitude. The cumulated yield (in mm) on the ridge represents 42% of the cumulated yield (in mm) of the four small condensers. It is only for the smallest yields that the large condenser gives larger values than the planar condensers.

The COG was inspected on several occasions early in the morning. A certain amount of water remained trapped up in the folds of the plastic foil on the surface of ridges and along the central trough. Folds and wrinkles because the plastic originally hugging the insulation surface becomes somewhat loose with exposure. Also the soil surface on which the insulation boards sit can develop small (up to ~10 cm) depressions due to uneven settling of soil even though the surface was smoothed at the time of construction. It is not easily possible to estimate the amount of water that remains trapped and later evaporated, but it is an appreciable amount. In future it would be advisable to compact the ridge surface with heavy rollers or to use rigid sheets to make the condenser surface instead of thin film and foils. This will lead to an increased initial investment, but will ensure full draining. Polycarbonate sheets can be used which are also very durable.

Another matter that requires further theoretical investigation is whether the central trough (50 cm wide and 34 m long), over which the condensate drains, contributes to condensation as much as the sloping and quick-draining surface of the ridges (Fig. 3b, along AB, and CD). Again, visual inspection in early morning revealed that the trough has a layer of water on it when dew occurs. The layer is thicker over the lower portion and more so near the outlet. The flow path along the ridge surface (AB or CD) is 100 cm with a 30° slope; along the trough has a 15° slope. As the water emissivity is nearly zero in the atmospheric window, it appears reasonable to assume that the layer of water affects the radiative cooling processes over the central trough and consequently condensation. Each trough surface is 17 m^2, i.e. 170 m^2 for all ten troughs. This represents a significant 20% of the COG surface area. If it is assumed that the trough does not contribute to condensation, but only conveys it to the gutter, the output of the COG in 2007 (6545 L) is 9.6 mm, which is 58.2% of the small plane measuring units (16.5 mm).

As mentioned earlier, large working installations tend to yield less dew per unit area than small units. COR at the small nearby village of Sayara (Sharan et al., 2007c) yielded nearly half that of the smaller units placed nearby, the same ratio as in this study. The COG Panandhro yield was 41.8% less than the small units on the site. In addition to water, another plausible explanation appears to be the non-uniform temperature regime on the surface, as shown by simulation. That in turn appears to be caused by aerodynamics over the condenser field. Uniformity is greater when wind is from the front. Eddies and swirls over the rough condenser field require further investigation in future to help determine optimal scale-up (ridge length, width of walls A B and C D) for large working installations so as to bridge the gap in yields of small and large units. A useful explanation – difference in radiation budget – has been discussed by Muselli et al. (2006a) who found that an aerial framed condenser could have a better cumulated yield (+9%) than the same condenser built on the ground. This difference in yield could also be related to the acceleration of air free convection when enlarging the size of the condensing surface, an acceleration

Table 2
Monthly dew collection during 2007 from plane condensers and a ridge plant. No measurements were made in December.

Month (year 2007)	Plane north (mL)	Plane east (mL)	Plane south (mL)	Plane west (mL)	850 m^2 Ridges (L)
January	492	480	514	413	221
February	4305	4046	3925	4035	1860
March	4120	3950	3880	3840	1597
April	3505	3760	4010	3850	1620
May	835	705	950	730	262
June–September	0	0	0	0	0
October	1995	2030	2037	2035	585
November	1430	1435	1440	1445	400
December	–	–	–	–	–
Total	16,682	16,406	16,756	16,348	6545

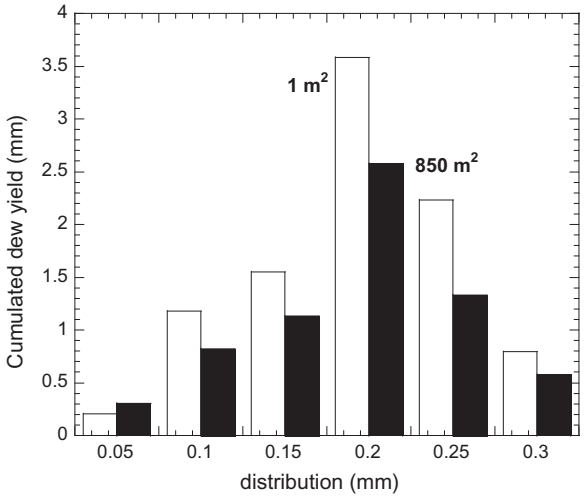

Fig. 11. Cumulated dew volumes (mL) corresponding to a given class of dew yield amplitude). Black bars: 850 m^2 condenser; white bar: mean yield from the four planar 1 m^2 condensers.

that reduces the cooling efficiency as already discussed in Section 3.3. This phenomenon has also been pointed out by Clus et al. (2006) when changing the scale and shape of condensers.

4.4. Water quality

Filtration was assessed at individual ridge outlets. The storage tank bottom was cleaned periodically to remove sediment. Water samples were analyzed in an accredited laboratory in Ahmedabad. The goal was not to make a thorough set of analyses but rather to decide whether dew water could fit Indian regulations for potable water quality and World Health Organization (WHO, 2011) recommendations. Samples were taken from the storage tanks made of HDPE (trade name SYNTEX). Samples in clean and sealed small glass bottles were brought to the city from the COG site and transferred to the laboratory within 24 h. Results (Table 3) of tests done in April 2006 showed that water fulfilled the above requirements for potability, except for pH that was found to be too low.

Total dissolved solids (TDS), which comprise inorganic salts (principally calcium, magnesium, potassium, sodium, bicarbonates, chlorides and sulfates) and small amounts of organic matter that are dissolved in water, was 660 mg/L. This amount is comparable to the total mineralization ≈0.77 EC = 770 mg/L value as deduced from the electrical conductivity $EC \approx 1000\ \mu S\ cm^{-1}$. This high level is presumably due to the high amount of dust in the vicinity of the mine as another large COG (600 m^2) built later at Satapar showed a lower TDS (155 mg/L). Note that a high concentration of dissolved solids is commonly found in dusty areas of arid and semi-arid areas such as in southern Morocco (Lekouch et al., 2011, found 560 mg/L). Total dissolved solids are probably the result of airborne marine dust and also the dust generated by mining activity. A detailed study is well beyond the scope of the present paper, but some guidelines can be found in e.g. Lekouch et al. (2010).

Coliform organisms were absent as solar UV during the day ensures permanent sterilization of the condensing surface.

4.5. Price of dew water

The total expenditure on COG at Panandhro was US$3100 with US$1000 for the condensing foil. The foil has to be replaced once after 4 years. Other components will probably last 15 years. Maintenance is periodic (once per week): sweeping of surface and any other place needed, clearing sediment filters and cleaning the storage tank (all done by the mining company). Water can be pouch-filled mechanically using a pouch-filling machine. Typically a 2000 pouch per hour machine costs US$2000. In 8 h about 20,000 pouches can be filled, with an electricity consumption of 4 kWh costing about 50 cents. Such machines have been in used in the area, are reliable, relatively low maintenance and can last 10–15 years. Then the cost of production for bottled water is in the order of US$520 per year, neglecting electricity consumption. The annual yield of dew water can be taken as 7000 L (in 2007 it was over 6500 but December data was not recorded), which is equal to 0.074 US$/L. As the market price of bottled water is about 0.22 US$/L in India, the present cost is thus only one-third.

It is useful to mention another important feature. The COG surface provides a ready-made highly efficient surface for rainwater collection. Annual rainfall of 100 mm is very likely to occur as the annual mean is around 200 mm. Accordingly, the rain collected from the COG during the four month rainy season (June–September) would be 85,000 L.

As there are long gaps between rain events and water is needed regularly for plantations, the mining company has been advised to build a holding structure near the COG with 20,000 L capacity. Large storage tanks made of HDPE (more than 20 year lifespan) would cost US$1200, increasing the annual cost to 580 US$. When rain water storage is added, and with the realistic assumption that rain water is potable, the total output from the COG during the

Table 3
Water quality parameters as compared to Indian permitted standards and the World Health Organization recommended guidelines.

Parameter	Unit	Analysis value	Maximum India permissible	Maximum WHO (recommended)
pH		4.74	6.5–8.5	9.5
Conductivity	μS/cm	1002	2880	No health-based guideline value
Color	CO-PT	2	25	No health-based guideline value; a maximum value of 15 is accepted
Odor		Agreeable	Agreeable	Agreeable
Turbidity	NTU	1	10	5
Total dissolved solids	mg/L	660	2000	1000
Total hardness	mg/L	480	600	500
Chlorides	mg/L	57	1000	250
Sulfates	mg/L	80	400	500
Fluorides	mg/L	0.87	1.5	1.5
Phenolphthalen alkalinity	mg/L	Not detectable	Not specified	Not specified
Total alkalinity	mg/L	60	600	Low alkalinity < 50mg/L as $CaCO_3$ Medium alkalinity 50–250 mg/L as $CaCO_3$ High alkalinity > 250 mg/L as $CaCO_3$
Acidity	mg/L	45	not specified	
MPN index/100 mL		<2	<2	
Coliform organisms		Absent	Absent	Absent

year would rise to nearly 100,000 L. The cost of bottled dew water becomes 10 times less expensive, about 0.006 US$/L, only 3% of the market price. In addition, such water will be available throughout the year and reduce strain on the groundwater aquifers.

5. Concluding remarks

Commissioned by a mining company, a 850 m^2 dew condenser-on-ground facility was built at their lignite project site near the sea coast. Building directly on the ground was preferred over building on roof or on frames. The condenser-field has a ridge and trough architecture, employed for the first time at such a large scale. The facility is also capable of collecting rain.

The construction of this large dew collector was designed to collect the maximum water at the lowest cost. Lower construction costs led to a ground condenser approach rather than an off-ground condenser, although ground condensers will have a lower dew yield. In the present study, the large surface condenser yielded only 42% of the extrapolated results from the small 1 m^2 planar condensers. Numerical simulations were used to estimate the effect of orientation with respect to wind direction. It appears that back winds would be the most favorable configuration for enhancing dew yields when taking into account the most frequent nocturnal wind speeds (1.5 m/s, average direction 210°). Such an arrangement would increase dew yields from 10% to 20% for wind speeds greater than 1 m/s. However, the orientation of the large dew collector faced NW (315°) because of the topography. It thus corresponds to a mismatch of about 100°, which also explains why the dew yield was lower than the average of the four small off- ground condensers that were exposed to different wind directions.

This large-scale dew and rain collector has already delivered an interesting amount of dew water. Simple techniques were developed for erecting it in the cheapest way, leading to a delivery price of bottled water close to US$0.07/L, which corresponds to 30% of the actual price of water found in the local market. This computation considers only the dew water output and is therefore conservative. As this dew condenser is also able to collect rain water, the water price goes down to 3% of the local water market. Because of its success, a second system has been constructed nearby in Satapar (Jamnager district), about 500 km south-east along the same coastline as Panandhro.

Acknowledgments

Funding for this work was received from the World Bank and the Gujarat Energy Development Agency, Baroda. We are extremely grateful to Mr. A.K. Shrivatava for managing this project in the GMDC Company and A. Ahmed for helping in field implementation. We also thank J. Ouazzani (Arcofluid company, France) for reviewing the CFD work and advice, and S. Berkowicz for a critical reading of the manuscript. PhD financial support for O. Clus was provided by the "Collectivité Territoriale de Corse", France.

References

Berger, X., Bathiebo, J., 2003. Directional spectral emissivities of clear skies. Renew. Energy 28, 1925–1933.
Berkowicz, S., Beysens, D., Milimouk, I. Heusinkveld, Muselli, M., Wakshal, E., Jacobs, A., 2004. Urban dew collection under semi-arid conditions: Jerusalem. In: Proceedings of the Third International Conference on Fog, Fog Collection and Dew, Cape Town, South Africa, October 11–15, 2004. Paper F2.
Beysens, D., 1995. The formation of dew. Atmos. Res. 39, 215–237.
Beysens, D., 2006. Dew nucleation and growth. C.R. Physique 7, 1082–1100.
Beysens, D., Milimouk, I., Nikolayev, V., Muselli, M., Marcillat, J., 2003. Using radiative cooling to condense atmospheric vapour: a study to improve water yield. J. Hydrol. 276, 1–11.
Beysens, D., Muselli, M., Nikolayev, V., Narhe, R., Milimouk, I., 2005. Measurement and modeling of dew in island, coastal and alpine areas. Atmos. Res. 73, 1–22.
Beysens, D., Ohayon, C., Muselli, M., Clus, O., 2006. Chemical and bacterial characteristics of dew and rain water in an urban coastal area (Bordeaux, France). Atmos. Environ. 40, 3710–3723.
Beysens, D., Clus, O., Mileta, M., Milimouk, I., Muselli, M., Nikolayev, V., 2007. Collecting dew to improve water resources: the D.E.W. project in Biševo (Croatia). Energy 32, 1032–1037.
Bird, R.B., Stewart, W.E., Lightfoot, E.N., 1960. Transport Phenomena. Wiley, New York, pp. 283–287.
Clus, O., 2007. Condenseurs radiatifs de la vapeur d'eau atmosphérique (rosée) comme source alternative d'eau douce. Université de Corse, France (PhD), p. 222.
Clus, O., Muselli, M., Beysens, D., Nikolayev, V., Ouazzani, J., 2006. Computational fluid dynamic (CFD) applied to radiative cooled dew condensers. In: Proceedings of the Fifth IEEE International Symposium on Environment Identities and Mediterranean area, Corte, France, July 2006.
Clus, O., Sharan, G., Singh, S., Muselli, M., Beysens, D. 2007. Simulating and testing a very large dew and rain harvester in Panandhro (NW India). In: Proceedings of Fourth International Conference on Fog, Fog Collection and Dew, La Serena, Chile, July 22–27, 2007.
Clus, O., Ortega, P., Muselli, M., Milimouk, I., Beysens, D., 2008. Study of dew water collection in humid tropical islands. J. Hydrol. 361, 159–171.
Clus, O., Ouazzani, J., Muselli, M., Nikolayev, V., Sharan, G., Beysens, D., 2009. Comparison of various radiation-cooled dew condensers by computational fluid dynamic. Desalination 249, 707–712.
Gandhidasan, P., Abualhamayel, H.I., 2005. Modeling and testing of a dew collection system. Desalination 180, 47–51.
Garratt, J.R., Segal, M., 1988. On the contribution of atmospheric moisture to dew formation. Bound.-Lay. Meteorol. 45, 209–236.
Guyer, E.C., Brownell, D.L., 1999. Handbook of Applied Thermal Design, first ed. Taylor and Francis.
Jacobs, A.F.G., Heusinkveld, B.G., Berkowicz, S.M., 2008. Passive dew collection in a grassland area, The Netherlands. Atmos. Res. 87, 377–385.
Lekouch, I., Mileta, M., Muselli, M., Milimouk-Melnytchouk, I., Šojat, V., Kabbachi, B., Beysens, D., 2010. Comparative chemical analysis of dew and rain water. Atmos. Res. 95, 224–234.
Lekouch, I., Muselli, M., Kabbachi, B., Ouazzani, J., Melnytchouk-Milimouk, I., Beysens, D., 2011. Dew, fog, and rain as supplementary sources of water in south-western Morocco. Energy 36, 2257–2265.
Monteith, J.L., 1957. Dew. Quart. J. Royal Meteorol. Soc. 83, 322–341.
Monteith, J.L., Unsworth, M.H., 1990. Principles of Environmental Physics, second ed. Chapman & Hall, New York.
Muselli, M., Beysens, D., Marcillat, J., Milimouk, I., Nilsson, T., Louche, A., 2002. Dew water collector for potable water in Ajaccio (Corsica Island, France). Atmos. Res. 64, 297–312.
Muselli, M., Beysens, D., Milimouk, I., 2006a. A comparative study of two large radiative dew water condensers. J. Arid Environ. 64, 54–76.
Muselli, M., Soyeux, E., Beysens, D., Clus, O., 2006b. Is dew potable? Study of the physical, chemical and biological dew characteristics in Ajaccio (France). J. Environ. Quality 35, 1812–1817.
Nikolayev, V.S., Beysens, D., Gioda, A., Milimouk, I., Katiushin, E., Morel, J.-P., 1996. Water recovery from dew. J. Hydrol. 182, 19–35.
Nikolayev, V.S., Beysens, D., Muselli, M., 2001. A computer model for assessing dew/frost surface deposition. In: Shemenauer, R.S., Puxbaum, H. (Eds.), Proceedings of the Second International Conference on Fog and Fog Collection, St John's (Canada), IRDC, July, pp. 333–336.
Nilsson, T., 1996. Initial experiments on dew collection in Sweden and Tanzania. Sol. Energy Mater. Sol. Cells 40, 23–32.
OPUR, International Organization for Dew Utilization. <www.opur.u-bordeaux.fr>.
Pal Arya, S., 1988. Introduction to Micrometeorology. Academic Press, San Diego.
Sharan, G., 2006. Dew Harvest to Supplement Drinking Water Sources in Arid Coastal Belt of Kutch. Foundation Books, Centre for Environmental Education, India.
Sharan, G., Prakash, H., 2003. Dew condensation on greenhouse roof at Kothara. J. Agric. Eng. 40, 75–76.
Sharan, G., Beysens, D., Milimouk, I., 2007a. A study of dew water yields on galvanized iron roof in Kothara (North-West India). J. Arid Environ. 69, 259–269.
Sharan, G., Shah, R., Millimouk-Melnythouk, I., Beysens, D., 2007b. Roofs as dew collectors: I. Corrugated galvanized iron roofs in Kothara and Suthari (NW India). In: Proceedings of Fourth International Conference on Fog, Fog Collection and Dew, July 22–27, La Serena, Chile.
Sharan, G., Singh, S., Millimouk-Melnythouk, I, Muselli, M., Beysens, D., 2007c. Roofs as dew collectors: III. Special polyethylene foil on a school in Sayara (NW India). In: Proceedings of Fourth International Conference on Fog, Fog Collection and Dew, July 22–27, La Serena, Chile.
WHO, 2011. Draft third edition of the WHO Guidelines for Drinking-Water Quality. <http://www.who.int/water_sanitation_health/dwq/guidelines3rd/en/>.